

Possible quantitative measures of order/disorder in models of liquid and amorphous structures

This article has been downloaded from IOPscience. Please scroll down to see the full text article.

1994 J. Phys.: Condens. Matter 6 10939

(<http://iopscience.iop.org/0953-8984/6/50/006>)

View [the table of contents for this issue](#), or go to the [journal homepage](#) for more

Download details:

IP Address: 171.66.16.179

The article was downloaded on 13/05/2010 at 11:32

Please note that [terms and conditions apply](#).

Possible quantitative measures of order/disorder in models of liquid and amorphous structures

Orsolya Gereben, László Pusztai and András Baranyai

Laboratory of Theoretical Chemistry, L. Eötvös University, Budapest 112, POB 32, H-1518. Hungary

Received 19 July 1994, in final form 15 September 1994

Abstract. The variance of the pair correlation function, the triplet correlation function, $g^{(3)}(r, s, t)$, and the three-body contribution to the configurational entropy, S_3 , were studied as possible tools for distinguishing between three different models of amorphous silicon (a-Si) with (nearly) identical pair correlation functions. All of these quantities were shown to be able to make the distinction unequivocally. For practical reasons, short-range S_3 is suggested as the best quantitative measure of disorder, in terms of higher-order correlations. For the first time, various projections of the three-body correlation function of a complicated amorphous material are also shown. On the basis of the current study it is proposed that the most realistic structural model of a-Si is the reverse Monte Carlo fit, starting from the well known Wooten model.

1. Introduction

If the atoms of disordered systems (liquids or glasses) interact via spherically non-symmetric pair forces the information provided by the measured spherically symmetric structure function or pair-correlation function is incomplete. In the case of systems consisting of one atomic species only, one needs three independent variables to describe the mutual positions and orientations of two particles in order to calculate their interaction energy. Then the same number of independent variables is necessary to characterize the resulting structure at the level of pair correlations. This lack of information can be even more severe in the case of multicomponent or molecular systems. If one counts the number of independent variables (N_i) necessary to define unequivocally the relative arrangements of two molecules the result is usually much bigger than the number of partial pair-correlation functions (N_p) available from experimental data. Our present example, amorphous silicon, is a one-component material, where $N_i > N_p$. For these systems it is usually easy to reproduce the structure function by a reverse Monte Carlo (RMC) simulation [1]. Moreover, one has large freedom to introduce constraints based on chemical or physical evidence into the calculations. The resulting three-dimensional structures represent possible models of the real system. In such cases a detailed account must be given of how the simulation was performed in order to make this calculation verifiable. Although this approach seems fair, it suffers from serious deficiencies. First, if one shows a set of possible models for a system then it must be ensured that this set is complete, or at least as complete as possible, i.e. that it is impossible to build any other three-dimensional model with the same pair structure but significantly different higher-order structure. This requirement is mandatory, because no matter how cautious are our conclusions the reader may think of the present models as the probable structures of the system.

It is obvious that the most disordered model can be obtained from RMC calculations if one applies only point particles with no further constraint. This simulation will reproduce the structure function with as random a higher-order structure as possible, so this is the model with the highest configurational entropy. How can one find the other end, the most ordered structure, with the same pair structure? Evidently, this search requires a well defined *measure* that can quantify the differences between various models, based on the level of disorder they represent. Once such a measure has been established, one can search for specific minimization techniques providing the two extrema of this scale. Certainly we do not claim that any of the measures proposed in the following would be capable to select the *real* three-dimensional structure. However, knowing the most ordered and most disordered phases corresponding to a certain pair structure, all the possible models could be presented. This paper is devoted to the task of finding the most appropriate measure of structural order/disorder. We use amorphous silicon as an example.

Amorphous silicon (a-Si) was shown to have many structural models that are consistent with the experimental data [2, 3]. It is because of this property that a-Si was chosen to be the model system of the present study: it would be of great interest if any of the models could be supported on a quantitative physical basis. It will also be attempted to name the model that most probably represents the real structure.

The different structural models were produced by the reverse Monte Carlo method. The basic RMC algorithm has been described elsewhere in detail [1, 4, 5]. In short, RMC moves particles around randomly in the simulation box in order to reproduce a given set of diffraction data within the experimental uncertainties. Instead of minimizing the potential energy, particle moves are accepted or rejected depending on whether the new position gives rise to an improved agreement between experimental and calculated structure functions. Thus the result of an RMC calculation is a (set of) particle configuration(s) that is consistent with the experimental results. These configurations can later be analysed geometrically (see, for example, [4]).

2. Theory

Structural models having identical pair correlation functions can only be distinguished by their higher-order correlations. The next member of the correlation function hierarchy is the triplet correlation function, $g^{(3)}(r, s, t)$. For a one-component system containing structureless particles (spherically symmetric atoms) this function has three independent variables. At present, computer capacities make it impossible to go beyond this level. (The quadruplet correlation function needs at least six independent variables.) In fact, even the three-body correlations are difficult to handle.

Recently, Baranyai and Evans developed a direct method for calculating the entropy of classical fluids at equilibrium [6]. The method is based on a systematic expansion of the entropy in terms of the partial N -particle distribution functions given first by Green for the canonical ensemble [7] and subsequently by Nettleton and Green [8] and Ravechè [9] for the grand canonical ensemble. Baranyai and Evans showed that the form of the grand canonical expansion is in fact a local expression and an ensemble-invariant form. To see the convergence of the method the same authors developed a method to calculate and integrate the entire three-particle correlation function [10]. In disordered systems, where the range of the correlations is limited, the pair and triplet entropies, S_2 and S_3 , get no contributions from distant neighbours. The entropy contributions have an asymptotic value, which can quantify the disorder at the levels of pair and triplet correlations. The different structural

models from RMC calculations have nearly identical pair correlation functions so their pair entropy contributions are also nearly identical. At the level of triplet correlations, however, this is not the case. The different three-particle entropies quantitatively characterize the disorder in RMC configurations. This was shown in a preliminary communication [11] for the case of a-Si.

We can find other measures for characterizing the structure of RMC configurations. If one does not want to go into the realm of higher-order correlations then the necessary information should somehow be deduced from lower-order correlations. As RMC simulations provide complete knowledge of the three-dimensional structure this task is clearly manageable. A very important requirement in this respect is that the advocated quantity should be easily computable. The pair correlation function can be unambiguously given at every instant around each particle as a centre. In fact, the $g^{(2)}(r)$ of the system is the average of these individual functions. We can easily calculate the variance of these individual $g(r)$:

$$\Delta g^{(2)} = \frac{\sum_{i=1}^{n_r} \sum_{j=1}^{n_p} (g_j(r_i) - \bar{g}(r_i))^2}{n_r n_p} \quad (1)$$

where n_r is the number bins of the $g(r)$ histogram, and n_p is the number of particles, i.e. the number of individual pair correlation functions.

If our system was a perfect one-component crystal then every particle would possess perfectly identical individual $g(r)$. (With more components, or in more complicated cases, there were a small number of different individual $g(r)$, depending on the type and/or location of the central atom. At present we consider simpler systems only, as the principles are the same; only the number of individual $g(r)$ would be greater, making the investigation less transparent.) Thus the variance would be zero. On the other hand, if our system were a perfect gas the variance would be a maximum. (Since, in practice, we are talking about histograms consisting of a finite number of bins rather than continuous functions, the actual value would be a function of the bin size used in the calculation.) The same idea can be applied to any easily computable structural function. It is plausible to assume that the higher variance will always belong to the more disordered models. The only problem with this method is that the actual numerical value of the variance will be a function of the bin size. The bin size problem is related to the poor statistics of individual $g(r)$. There may be cases when only a very few particles, or even none, will get into a bin. Therefore, comparison between different systems cannot be made trivially. The method is not absolute in this sense. This problem can only be circumvented if we partition the sample into regions where the number of centres is sufficiently large to decrease substantially the bin size dependence. However, if these regions are too large it is very difficult to detect reliably the difference in the variances.

Another possibility is to approximate the entropy fluctuations. From thermodynamics [12]

$$\langle (\Delta S)^2 \rangle = C_p \quad (2)$$

where C_p is the isobaric heat capacity. Since close to the triple point at least 95% of the excess entropy is given by the two-particle contribution, it is plausible to assume that a similar behaviour may also be experienced in terms of the fluctuations. In such a way, in principle we could approximately connect a simulated property of the model to a measurable property of a real system.

3. Computational details: model systems

Three structural models of a-Si were produced and were then analysed. Two of the models were identical to those introduced earlier [2, 3]. The first is the result of an unconstrained RMC calculation, i.e. when no assumptions for the presence of tetrahedral bonding are imposed. This model will be denoted as U . The second model is an RMC fit where all the atoms are required to have exactly four neighbours. The starting configuration in this case is a diamond lattice, and the calculation is carried out in r space (fitting $g(r)$ of the U model). This model will be denoted as C .

In the third RMC calculation every atom again has strictly four neighbours, but the starting configuration is a relaxed tetrahedral network known as the Wooten model [13]. The main attraction of the resulting structure is that among all the constrained models considered (also among those in [2, 3]) it possesses the structure factor that is the closest to experimental results. Throughout the current study this model will be denoted as W .

For the U and C models systems with 216 particles were used, whereas the W model contained 1728 atoms. The larger system size was applied because that calculation applied Q space information (the structure factor) as input function, since the properties of the W model had not been known before. (Comparing models of different sizes did not influence our conclusions, since the range of the investigations was always well within the smaller box.) All three models contained 100 independent-particle configurations, which were collected during the reverse Monte Carlo calculations after careful equilibration. The interval between two independent configurations was always at least N accepted moves (where N is the number of particles).

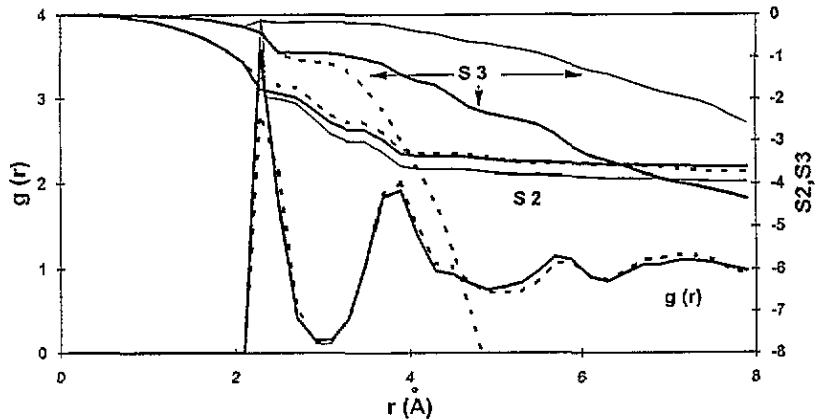


Figure 1. Pair correlation functions S_2 and S_3 for the three models. Full curve: U ; heavy full curve: W ; broken curve: C . The spacing (bin size) is 0.2 \AA in each case.

4. Results and discussion

The pair correlation functions, as well as the two- and three-body contributions to the configurational entropy, are shown in figure 1. The RMC simulations were carried out using $d_r = 0.1 \text{ \AA}$ when evaluating (or fitting) $g(r)$. In order to improve statistics at the three-body

level this spacing was doubled, so that every curve in figure 1 was calculated by using a different ($d_r = 0.2 \text{ \AA}$) binsize. This minor alteration (between the RMC procedure and the evaluation) could cause the small differences in terms of $g(r)$ at the first peak. The discrepancies are small and concentrated mainly on one single point, so that they are not significant from the point of view of the main objective of this work.

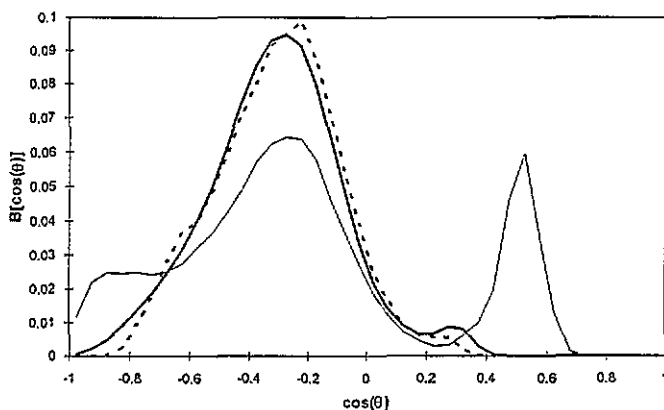


Figure 2. Cosine distribution of bond angles for the three models. Full curve: U ; heavy full curve: W ; broken curve: C .

The usual means of revealing higher-order structural characteristics is the distribution of cosines of bond angles, $B(\cos \Theta)$ (see, for example, [2]; it is a possible projection of the three-particle correlation function that is taken over all the possible angles formed by three atoms within the first coordination shell). Cosine distributions of bond angles for all three structural models of a-Si are shown in figure 2. Model U can clearly be separated from the other two models since the corresponding distribution has a large peak at around 60° ($\cos \Theta = 0.5$). However, models C and W cannot be distinguished on the basis of their $B(\cos \Theta)$ functions, although the different ways they had been produced suggest that they are different. To make the distinction, more sophisticated tools are needed.

4.1. The variance of $g^{(2)}(r)$

According to (1), $\Delta g^{(2)}$ values were calculated for the three models, using two different bin sizes in each case. As an attempt to eliminate the high statistical uncertainties at low r , up to first minimum of the PCF, the variance of the $4\pi r^2 g(r)$ function was also calculated. A summary of the results is given in table 1.

The first observation is that, independently of the type and spacing of the function, there is a clear tendency in each case towards increasing fluctuations, i.e. towards decreasing structural ordering in the order of models C , W , U . This order fulfills commonsense expectations. It is therefore suggested that the variance of either of the above two functions can be used as a simple quantitative measure of disorder for distinguishing different structural models of a given material (corresponding to the same data set), provided that identical bin size is used.

The multiplication by $4\pi r^2$ does not lead to an improved distinction between models, so only the quantity defined by (1) will be considered from now on. As is evident from table 1, the actual value of $\Delta g^{(2)}$ depends considerably on the bin size applied when calculating

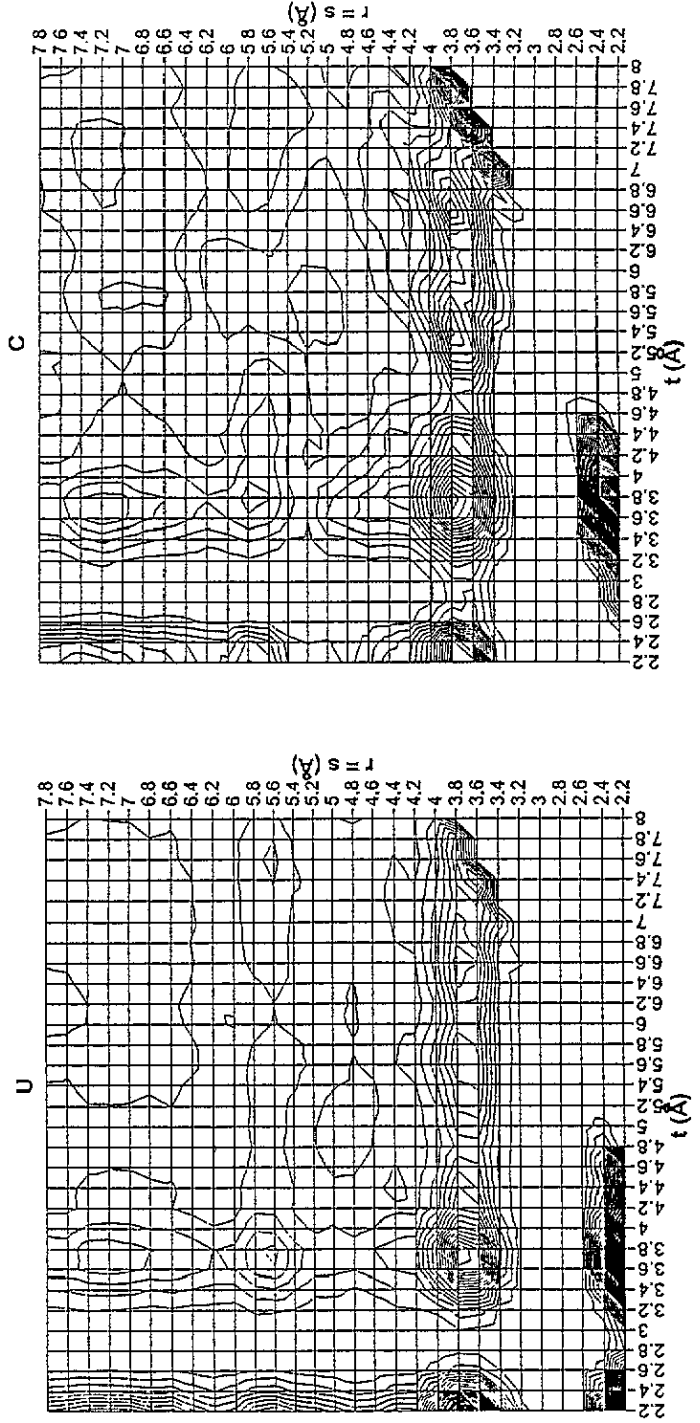


Figure 3. Isosceles projections of $g^{(3)}(r, s, t)$ for models U (left) and C (right).

the pair correlation function. As could be expected, using the larger bin size means a somewhat better (although not significantly better) distinction between different levels of disorder. Looking at the numbers reveals that there is a rather high level of basic noise in the fluctuations, which is responsible for about 90% of the values quoted. Compared with this noise, the differences between $\Delta g^{(2)}$ of the models are quite low. This unfortunate feature makes the prospective use of $\Delta g^{(2)}$ for characterizing structural disorder quantitatively somewhat inconvenient, although it was not possible to choose the parameters so that the above order of models would alter. The reliability of the method is also demonstrated by the values of uncertainties, which are well under 1% in all cases.

Considering the relatively small bin size dependence of the differences of $\Delta g^{(2)}$ it seems possible to use $\Delta g^{(2)}$ not only for comparing structural models of a given material, but also for comparing structural disorder in different materials. For this purpose the bin size used for the different measurements should somehow be standardized. It could, for instance, be scaled to a well defined point of the PCF. This point could be the position of the first maximum (or minimum). If the number of bins up to this point are equal then the purely statistical noise should have identical effects for the different cases. However, this way of quantitative comparison is suggested only for similar systems.

Knowing the values of $\Delta g^{(2)}$ for each of our models, the structures can be classified according to the extent of disorder. As was noted earlier, model *U* obviously seems the most disordered, whereas models *W* and *C* are more ordered, and model *W* is closer to model *C* than to model *U*.

Attempts were also made to compute $\langle(\Delta S)^2\rangle$ values, as they could be directly related to a well defined physical property (see (2)). However, $\langle(\Delta S)^2\rangle$ seemed to contain no additional information, and hence its use will not be further discussed here.

4.2. The three-particle correlation function, $g^{(3)}(r, s, t)$

The function $g^{(3)}(r, s, t)$, with r , s and t being the three position vectors of any particle triplet, is the full information that can be obtained on the correlation between the positions of three atoms. Thus it incorporates, for instance, the cosine distribution of bond angles (see figure 2). Since $g^{(3)}(r, s, t)$ has three independent variables, only projections of it can be shown explicitly. Since this is the first time when the full $g^{(3)}(r, s, t)$ (or in short, $g^{(3)}$) was calculated for a highly ordered system, several projections of it will be given in order to understand deeper structural differences or similarities.

In theoretical works [14, 15] projections for the equilateral ($r = s = t$) and the isosceles ($r = s, t$) configurations have been preferred, mostly because these are the ones that can be approximated, and also interpreted, more easily. For the sake of ease of comparison, isosceles projections are given in figure 3 for models *U* and *C*. (The pattern of model *W* is in between, and somewhat closer to that of model *C*.) This projection reveals correlations within given coordination spheres. In this way it is the closest relative to the cosine distribution of bond angles: every peak corresponds to a well defined angle, and the ends of the angles are in the same coordination shell.

The most apparent difference between the patterns is the presence (in model *U*) or the absence (in models *C* and *W*) of the peak at around $t = r = s = 2.3 \text{ \AA}$, which corresponds to 'close-packed'-like triplets (equilateral triangles with sides of about 2.3 \AA , i.e. of about the first neighbour distance.) These triplets are not present in the constrained models, as can also be seen in figure 2. The higher proportion of tetrahedral angles in models *C* and *W* are exhibited by the peak at $r = s = 2.3 \text{ \AA}$ and $t = 3.6 \text{ \AA}$. (This peak for model *C* is considerably higher than for model *U*, as shown by the number of contour lines.)

Table 1. Variances of $g^{(2)}(r)$ and $4\pi r^2 g^{(2)}(r)$ functions for the three structural models of a-Si.

Model	$\Delta g^{(2)}$			$\Delta(4\pi r^2 g^{(2)})$		
	$\Delta r = 0.1 \text{ \AA}$	$\Delta r = 0.2 \text{ \AA}$	$\Delta r = 0.1 \text{ \AA}$	$\Delta r = 0.1 \text{ \AA}$	$\Delta r = 0.2 \text{ \AA}$	$\Delta r = 0.2 \text{ \AA}$
U	$2.728 \times 10^{-4} \pm 1 \times 10^{-6}$	$1.791 \times 10^{-4} \pm 6 \times 10^{-7}$	$2.170 \times 10^{-3} \pm 2 \times 10^{-6}$	$1.882 \times 10^{-3} \pm 1 \times 10^{-6}$		
W	$2.660 \times 10^{-4} \pm 1 \times 10^{-6}$	$1.730 \times 10^{-4} \pm 5 \times 10^{-7}$	$2.169 \times 10^{-3} \pm 2 \times 10^{-6}$	$1.880 \times 10^{-3} \pm 2 \times 10^{-6}$		
C	$2.637 \times 10^{-4} \pm 1 \times 10^{-6}$	$1.716 \times 10^{-4} \pm 7 \times 10^{-7}$	$2.168 \times 10^{-3} \pm 2 \times 10^{-6}$	$1.878 \times 10^{-3} \pm 1 \times 10^{-6}$		

The isosceles (and equilateral) triplets ignore possible correlations between different coordination spheres. For investigating such correlations another type of projection was introduced. According to that, one distance (vector), which in our case is s , would be fixed, while the other two vectors would discover the entire subspace of (r, t) . In practice, this can be done by choosing two particles, which are the correct distance from each other, fixed, whereas the third particle could be any of the remaining ones. The rest of the projections of $g^{(3)}(r, s, t)$ shown in this work were made by using this sort of technique.

Figure 4 compares $g^{(3)}$ projections of the above type for the three models at four different (fixed) s values. Note that the symmetric (to the diagonal) nature of the patterns is not extraordinary but necessary. It would be sufficient to show either the upper or the lower part, with respect to the diagonal, of the figures. What is striking at first glance is that the patterns for the different models differ sharply. This is particularly so at higher distances. It is also apparent that all models, particularly model *C*, possess a rather substantial medium-range ordering over the second coordination shell. These $g^{(3)}$ projections are the first tools that can reveal this extended ordering. The peaks that correspond to the appropriate vector triplets can be connected to angles that are characteristic to distorted (to different degrees) tetrahedral lattices. This is true for all the three models, although naturally to different extents.

As a means of direct comparison of the models, $g^{(3)}$ of model *U* was subtracted from the $g^{(3)}$ of the other two models. The resulting 'difference' $g^{(3)}$ are shown in figure 5. It is remarkable that not only $g^{(3)}$ itself, but also the difference functions, are highly structured. All the peaks but the ones at around $r = t = 2.2 \text{ \AA}$ with $s = 2.2\text{--}2.4 \text{ \AA}$ are positive. This finding supports the expectation that models *W* and *C* are both more structured than model *U*, particularly at higher distances. It should also be noted that shifting towards higher s distances $g^{(3)}$ of $W - U$ seems to vanish. This suggests that the full $g^{(3)}$ of model *W* resembles more that of model *U* than that of model *C*. The longer-ranged almost crystalline-like structure of model *C* becomes intensely visible by these projections, which seem rather efficient in revealing such behaviour. (It should be remembered that model *C* had indeed been produced in a way that much of the crystalline nature could be reserved. There was not a single (covalent) bond switching involved, for instance.)

The full $g^{(3)}$ may not be the best tool for studying the extra correlations that are characteristic only to purely three-body effects since, at least among simple disordered systems like the Lennard-Jones fluid, many of the triplet correlations arise straightforwardly from the pair correlations [10]. In order to separate the genuine three-body contributions we have calculated $g^{(3)}(r, s, t)$ normalized by the product of the corresponding three $g^{(2)}$, i.e. by $g^{(2)}(r)g^{(2)}(s)g^{(2)}(t)$. Results for the three models of a-Si, in the s range of $2.2\text{--}2.8 \text{ \AA}$, are given by figure 6.

The most important observation is that, although this reduced $g^{(3)}$ for model *U* is less structured at the smallest distances, generally the reduction did not give rise to the smearing out of the features of the full $g^{(3)}$. The reduced $g^{(3)}$, however, emphasizes some features that are not apparent in the full $g^{(3)}$. The most obvious of these is the disappearance of the 'hard-sphere'-like peak of model *U* at $r = s = t = 2.3 \text{ \AA}$, that could therefore entirely be composed from single $g^{(2)}$. At the same time, peaks built up at $r = t = 2.8 \text{ \AA}$ (with $s = 2.2\text{--}2.4 \text{ \AA}$) in the reduced $g^{(3)}$ of model *U*, but particularly strongly, in that of model *W*. These peaks can be explained by knowing that $g^{(2)}(r)$ reaches its very low minimum value at about $r = 2.8\text{--}3.0 \text{ \AA}$. Dividing by this small value twice can cause the build-up of the peaks in question. In other respects, reduced $g^{(3)}$ of models *U* and *W* seem to possess similar degrees of structural ordering. This connects these two models more strongly than either of them to model *C*.

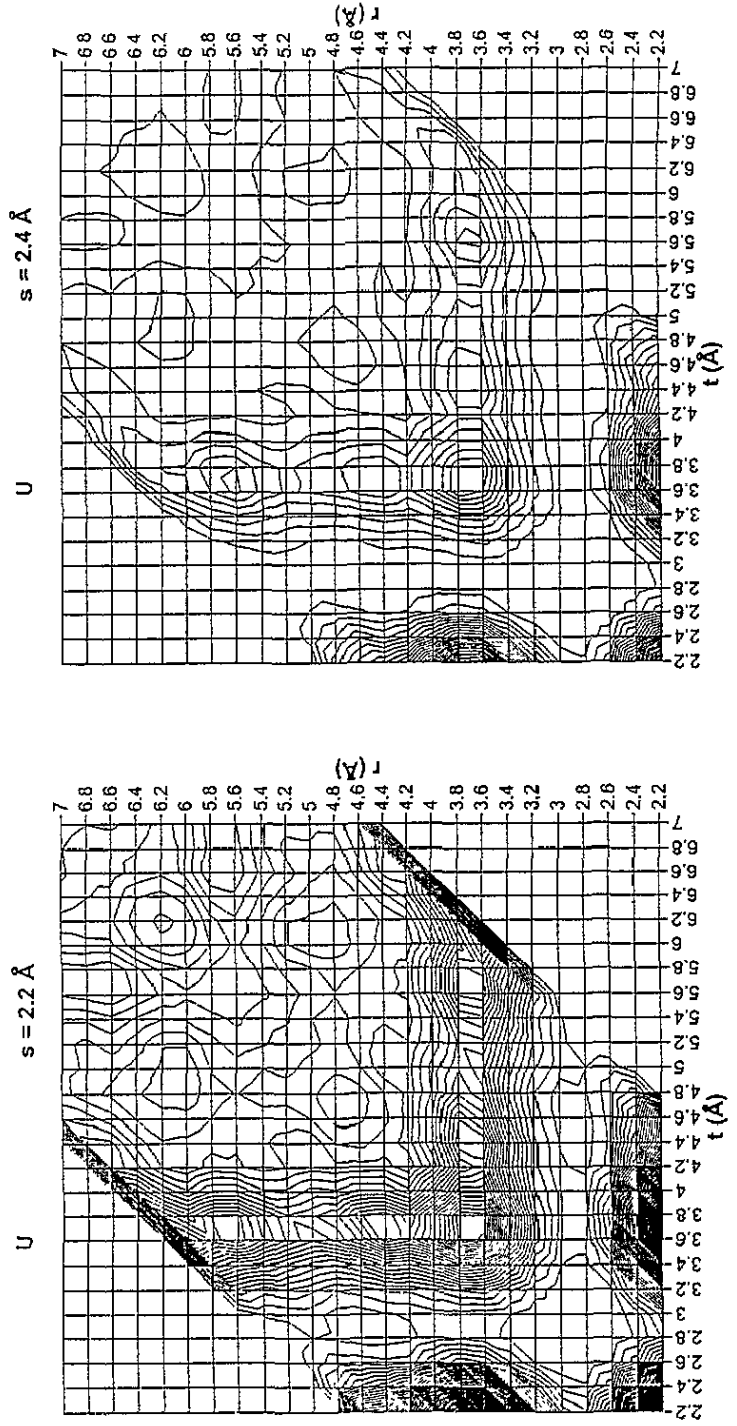


Figure 4. Two-dimensional projections of $g^{(3)}(r, s, t)$ with fixed s for the three models. ($\Delta_z = 0.5$ for $s = 2.2-2.4 \text{ \AA}$ and 0.1 otherwise. (The symmetrical nature is necessary.)

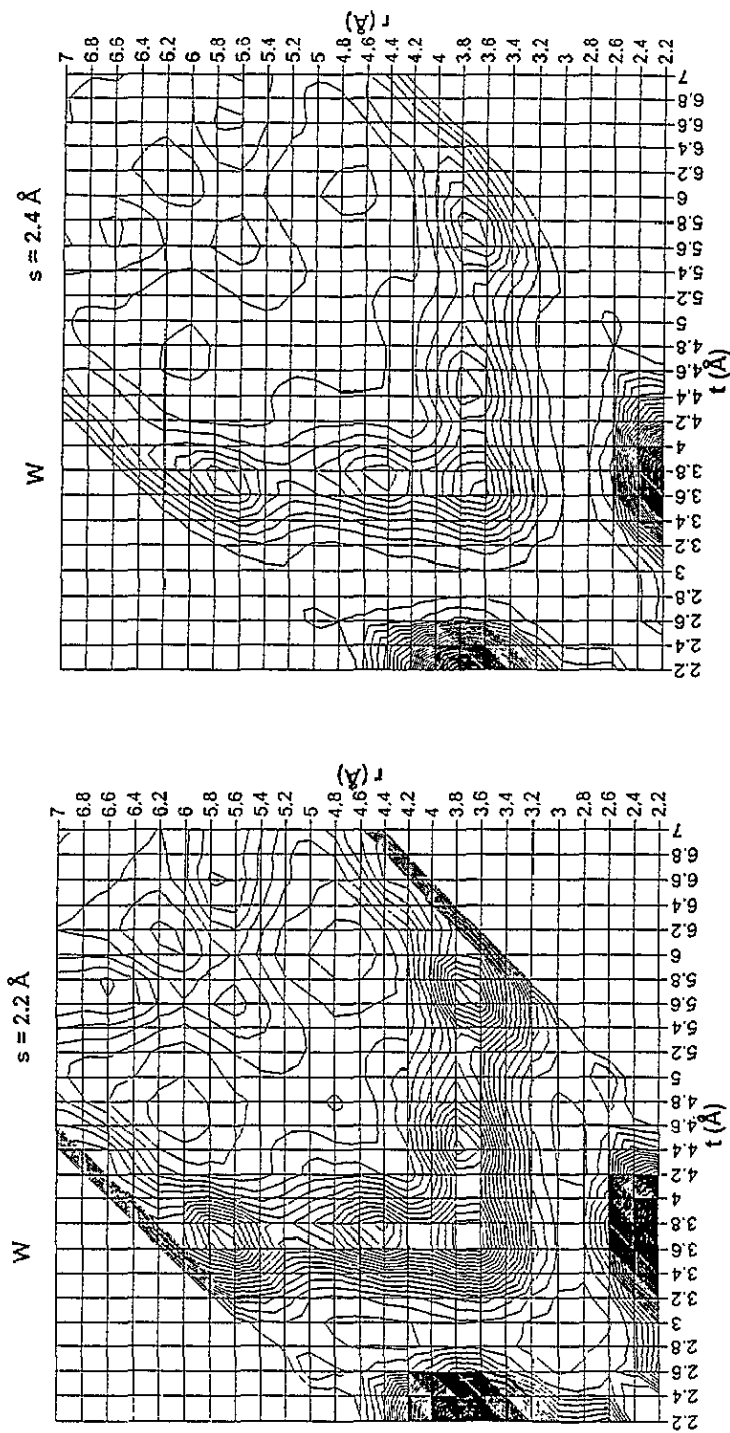


Figure 4. Continued.

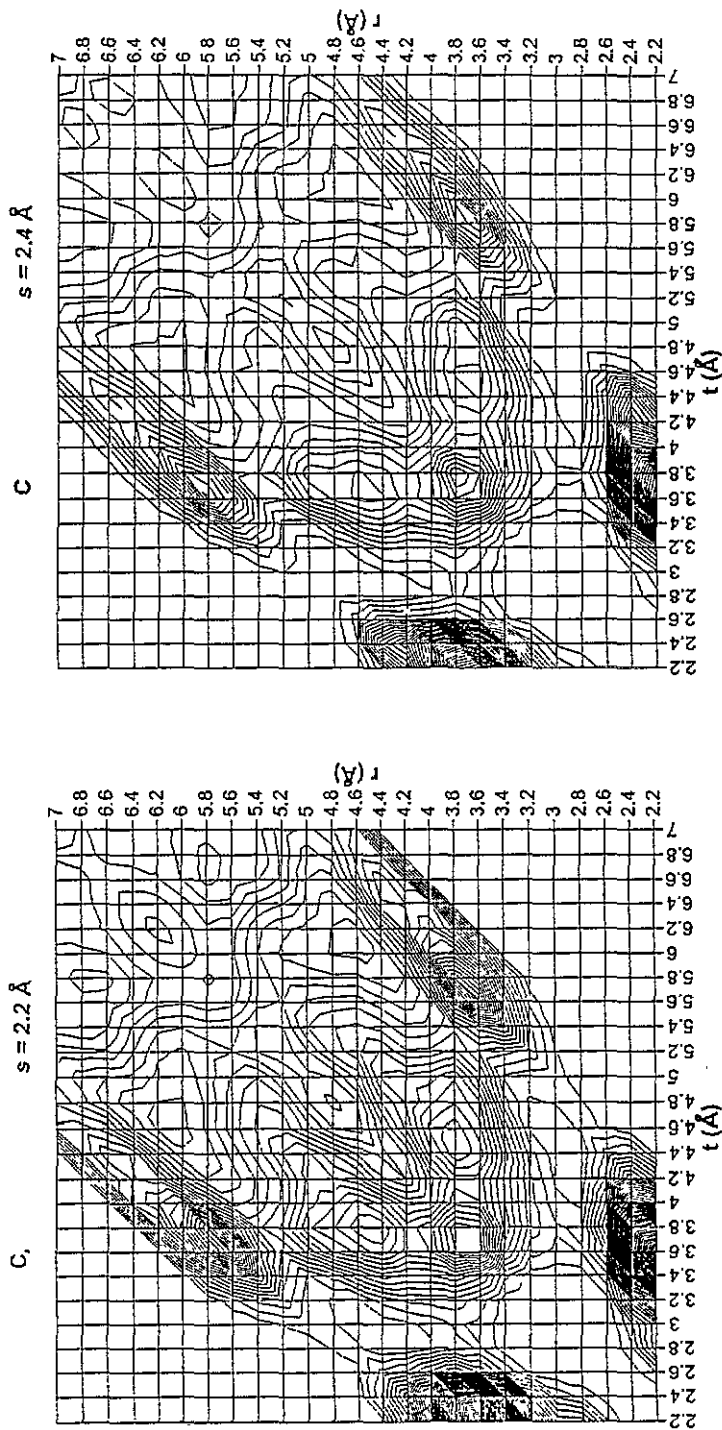


Figure 4. Continued.

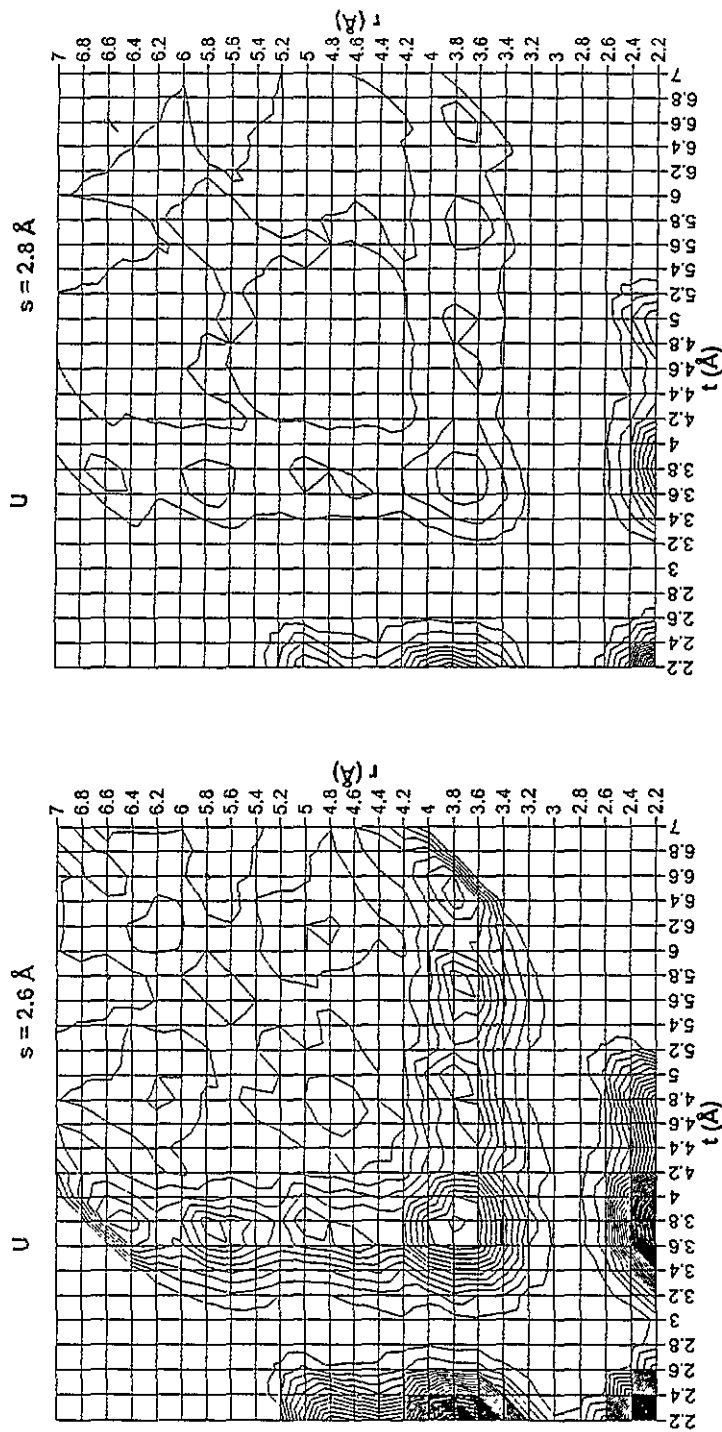


Figure 4. Continued.

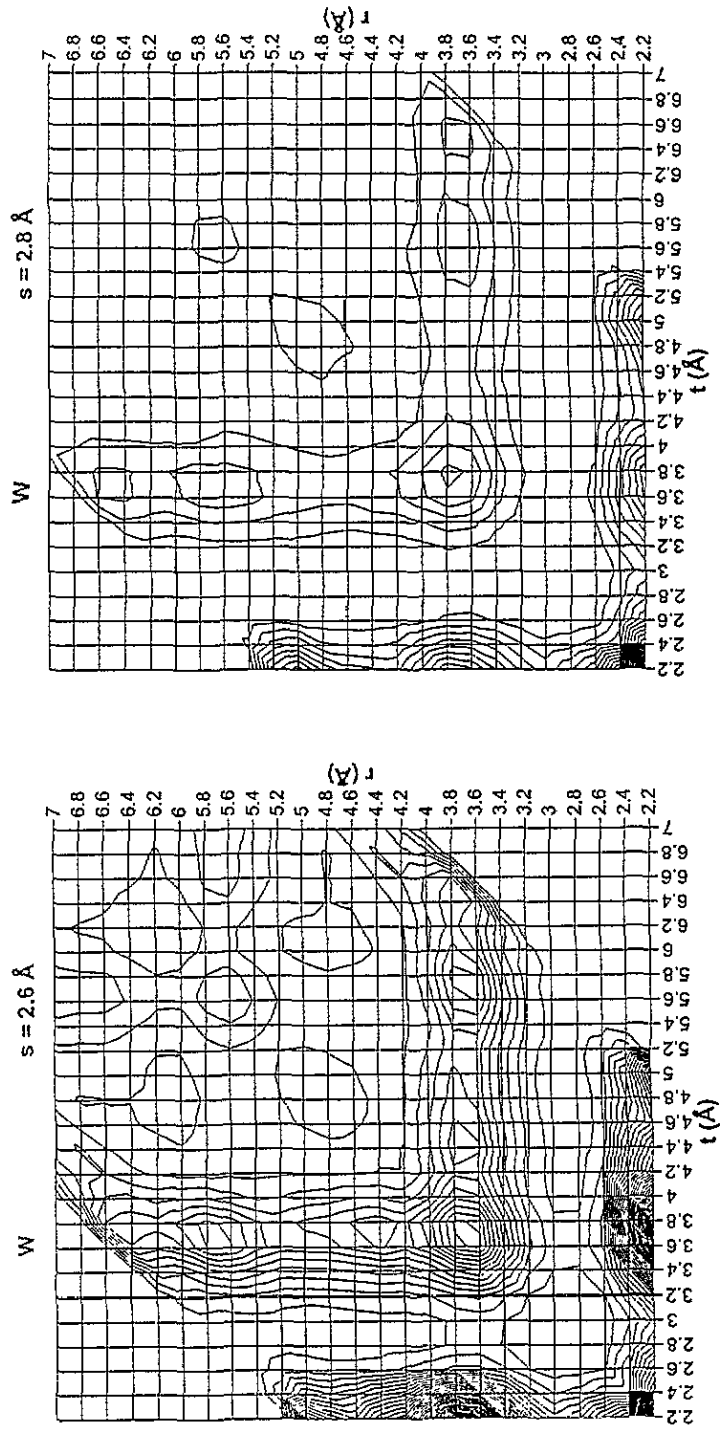


Figure 4. Continued.

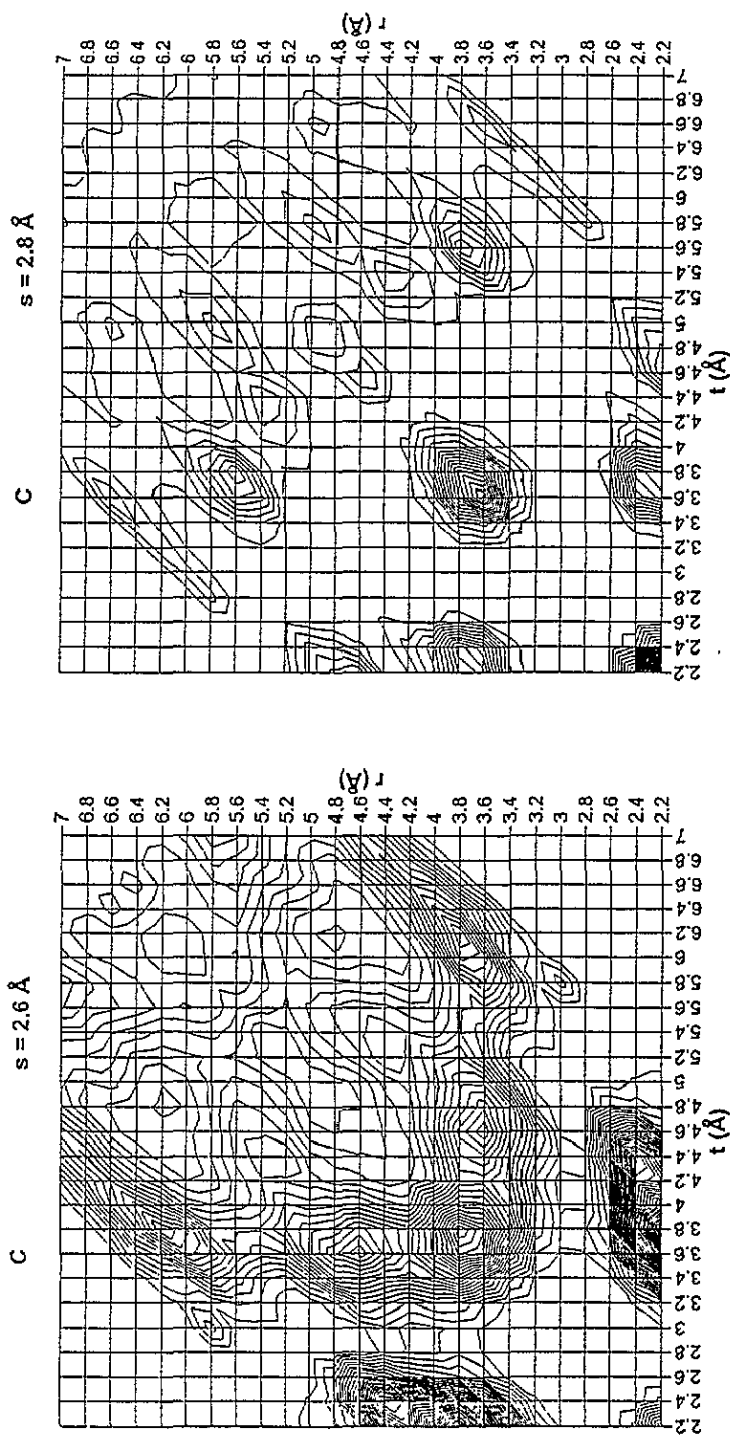


Figure 4. Continued.

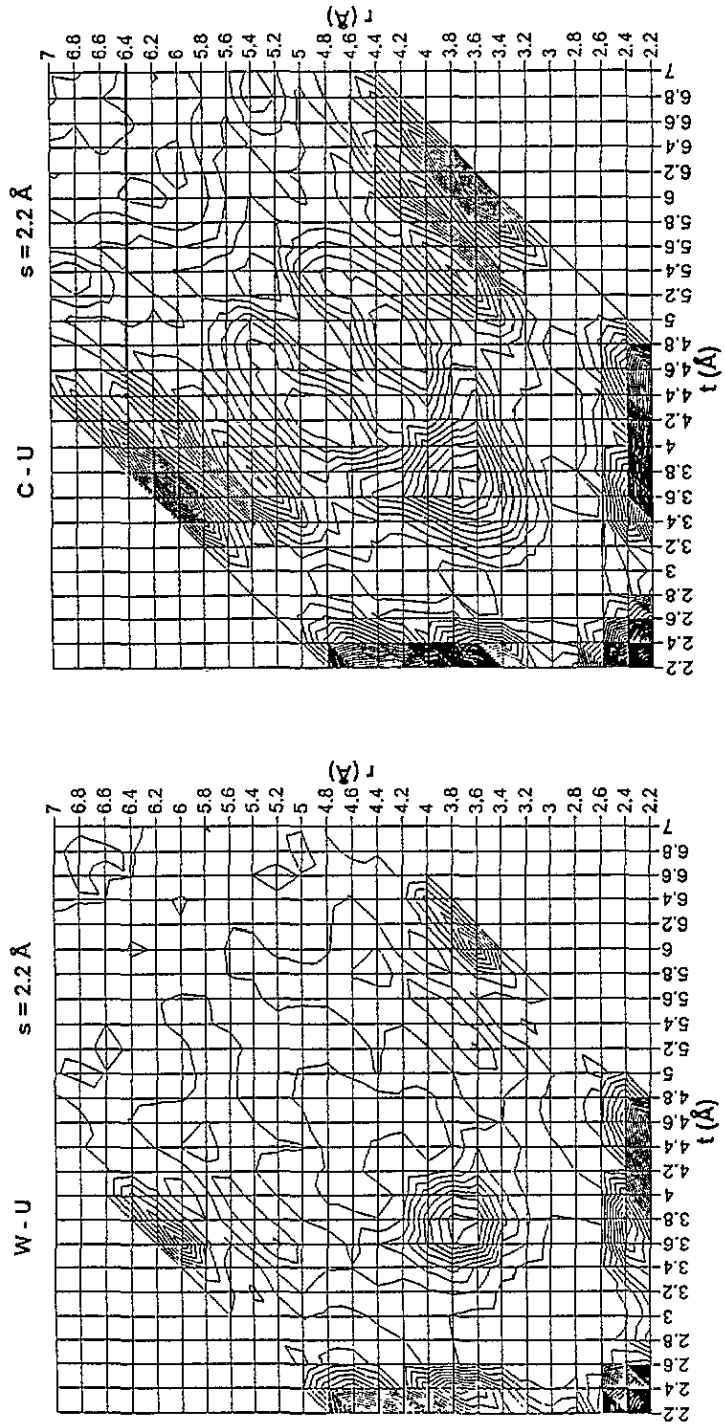


Figure 5. Two-dimensional projections of 'difference' ρ^B with fixed s for $W-U$ and $C-U$. $\Delta_z = 0.1$ for $s = 2.8 \text{ \AA}$, and 0.5 otherwise

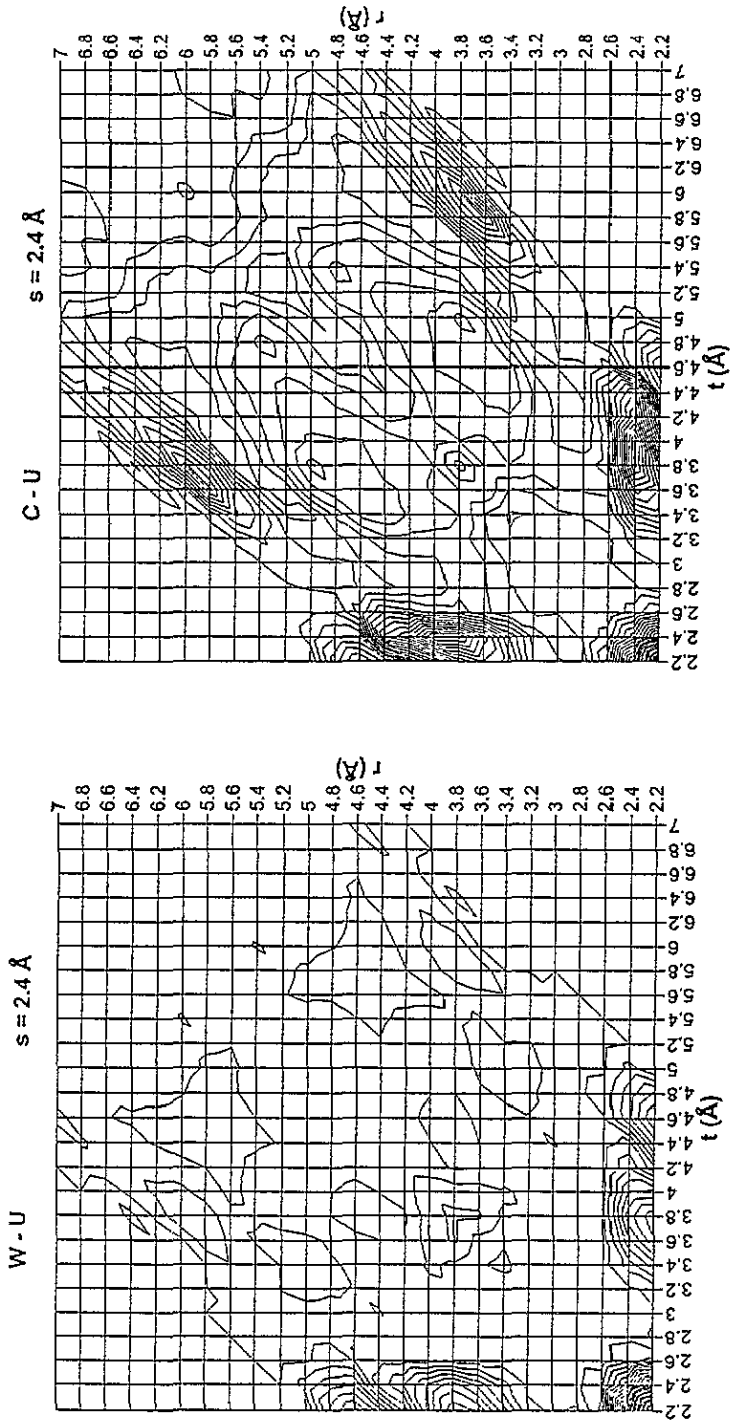


Figure 5. Continued.

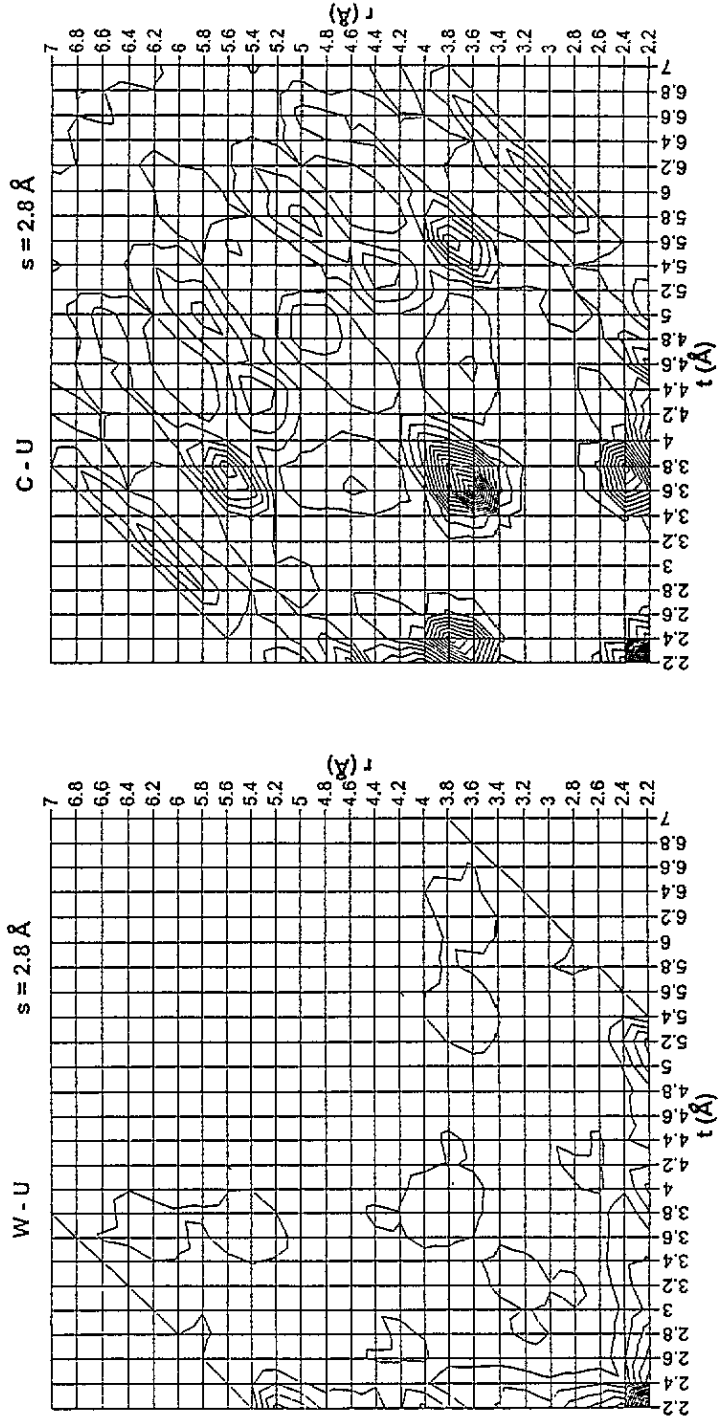


Figure 5. Continued.

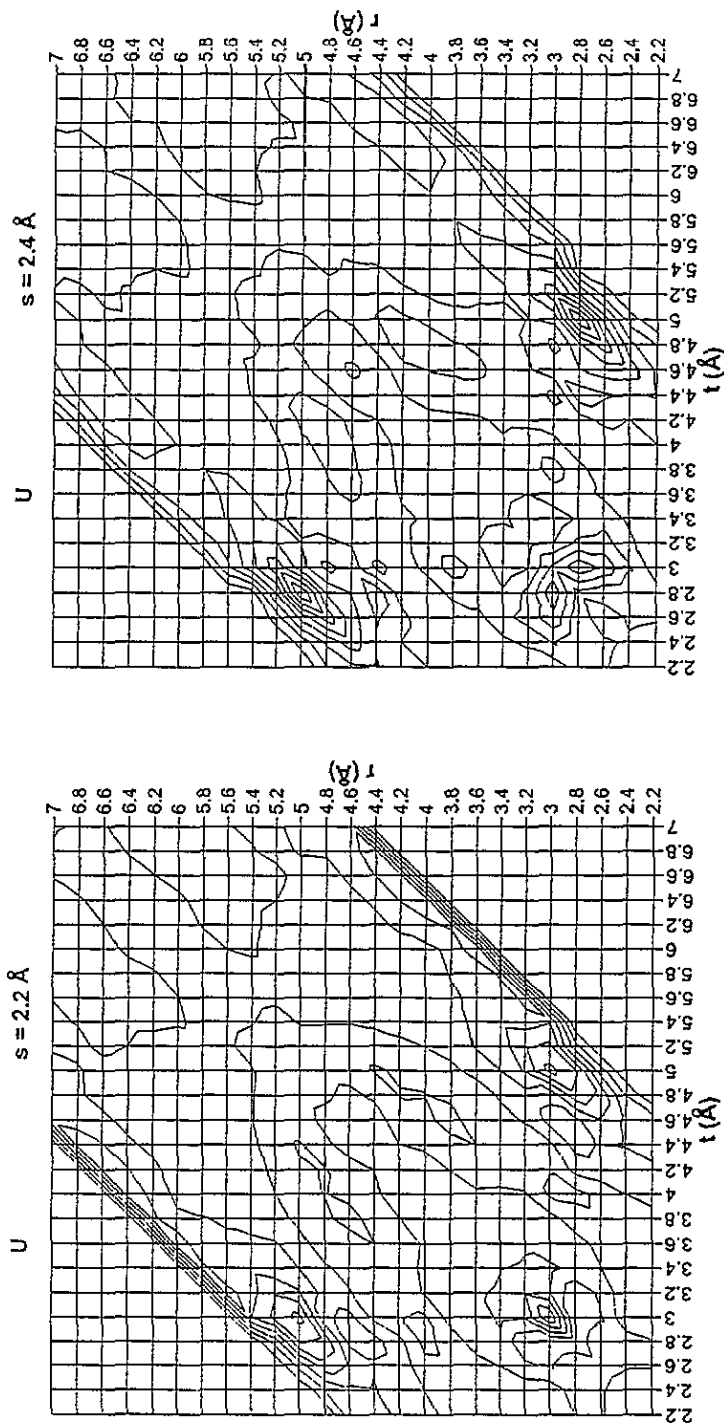


Figure 6. Two-dimensional projections of $g^{(3)}(r, s, t) / [\lg^{(2)}(r)g^{(2)}(s)g^{(2)}(t)]$ with fixed s for the three models. $\Delta_z = 0.25$.

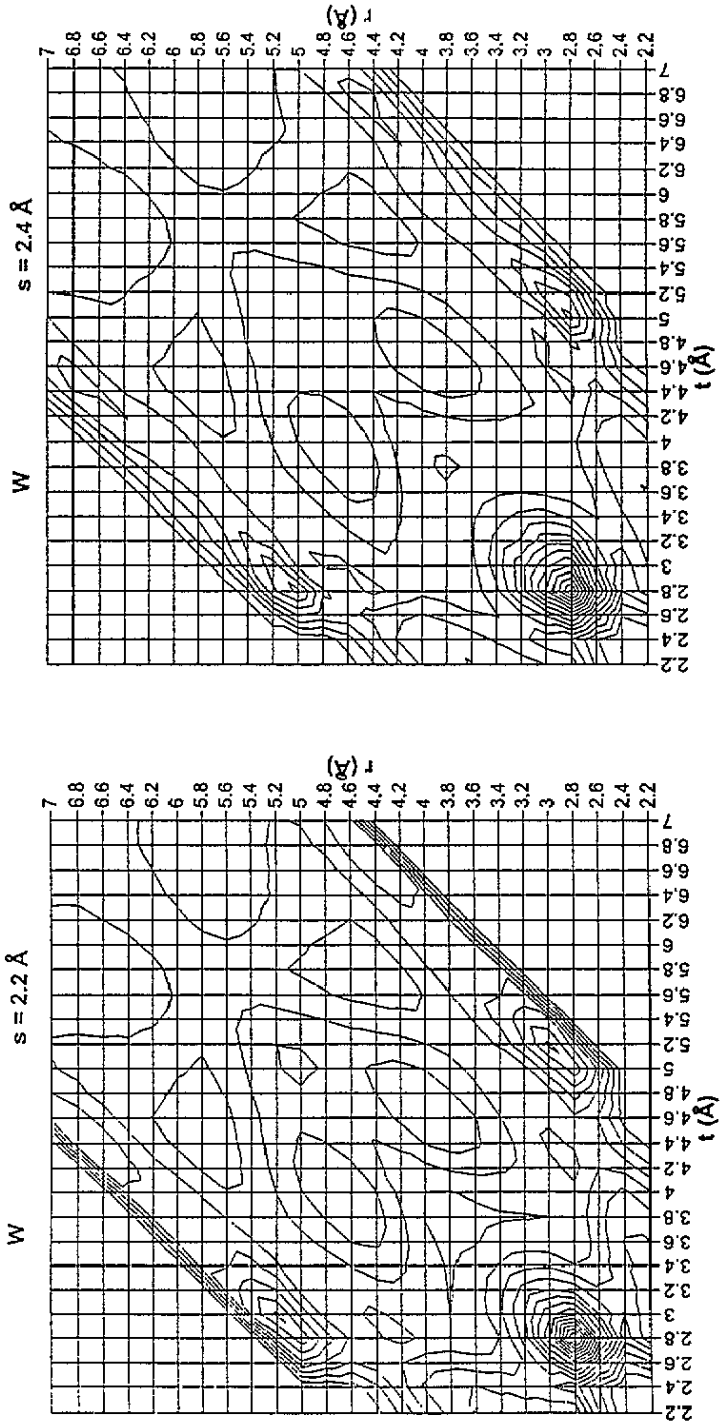


Figure 6. Continued.

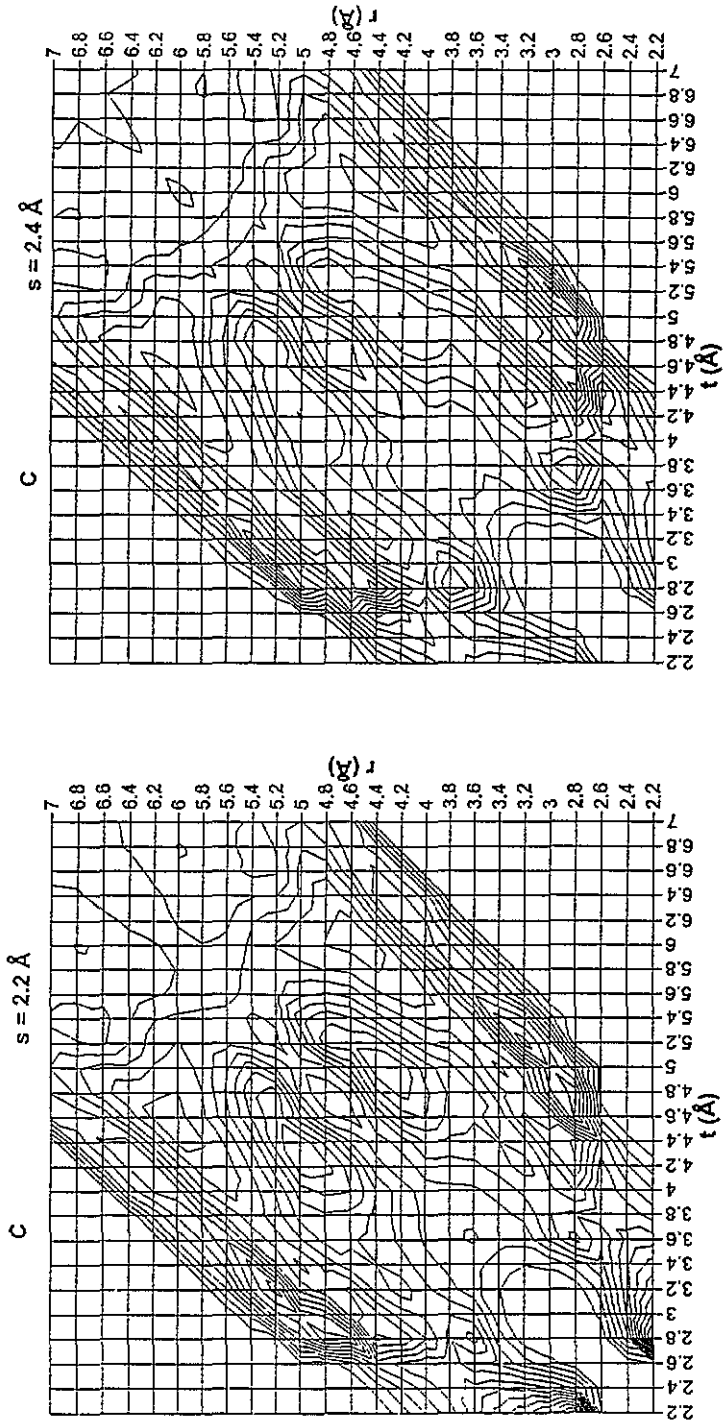


Figure 6. Continued.

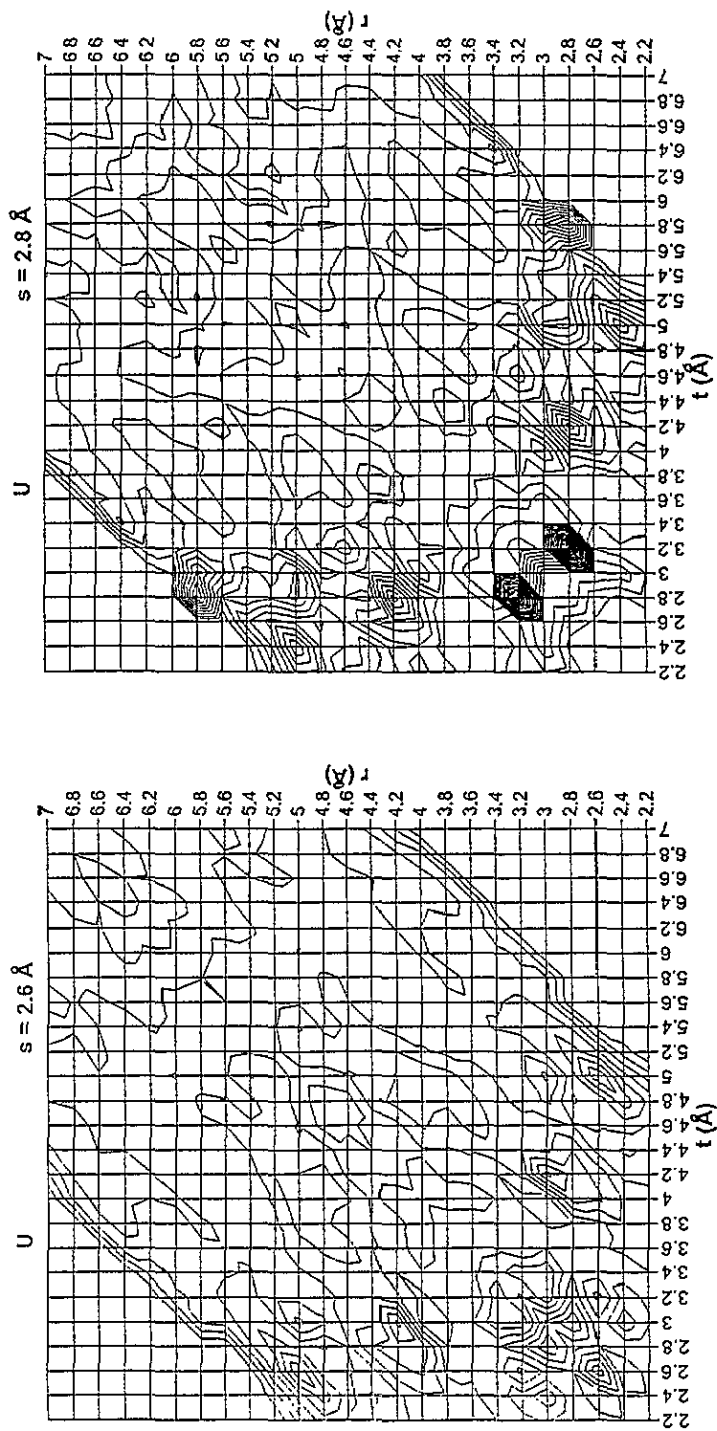


Figure 6. Continued.

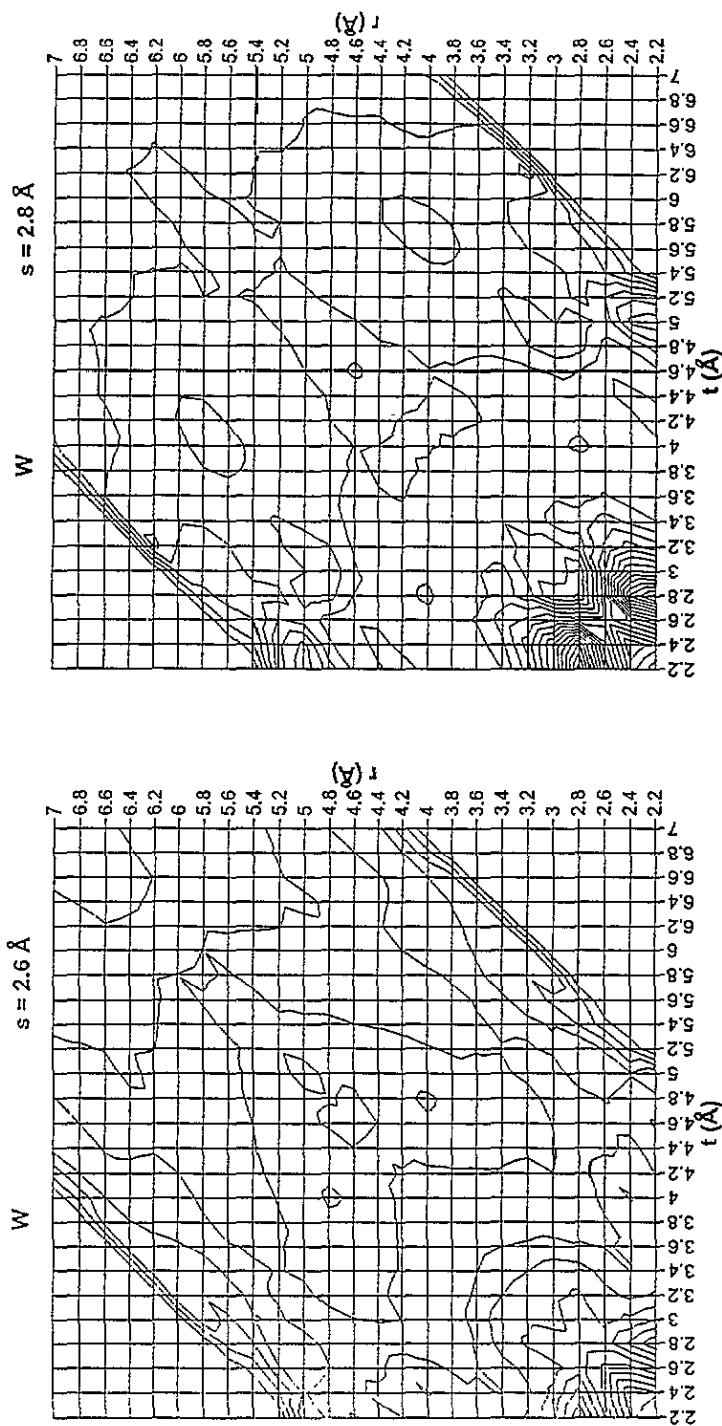


Figure 6. Continued

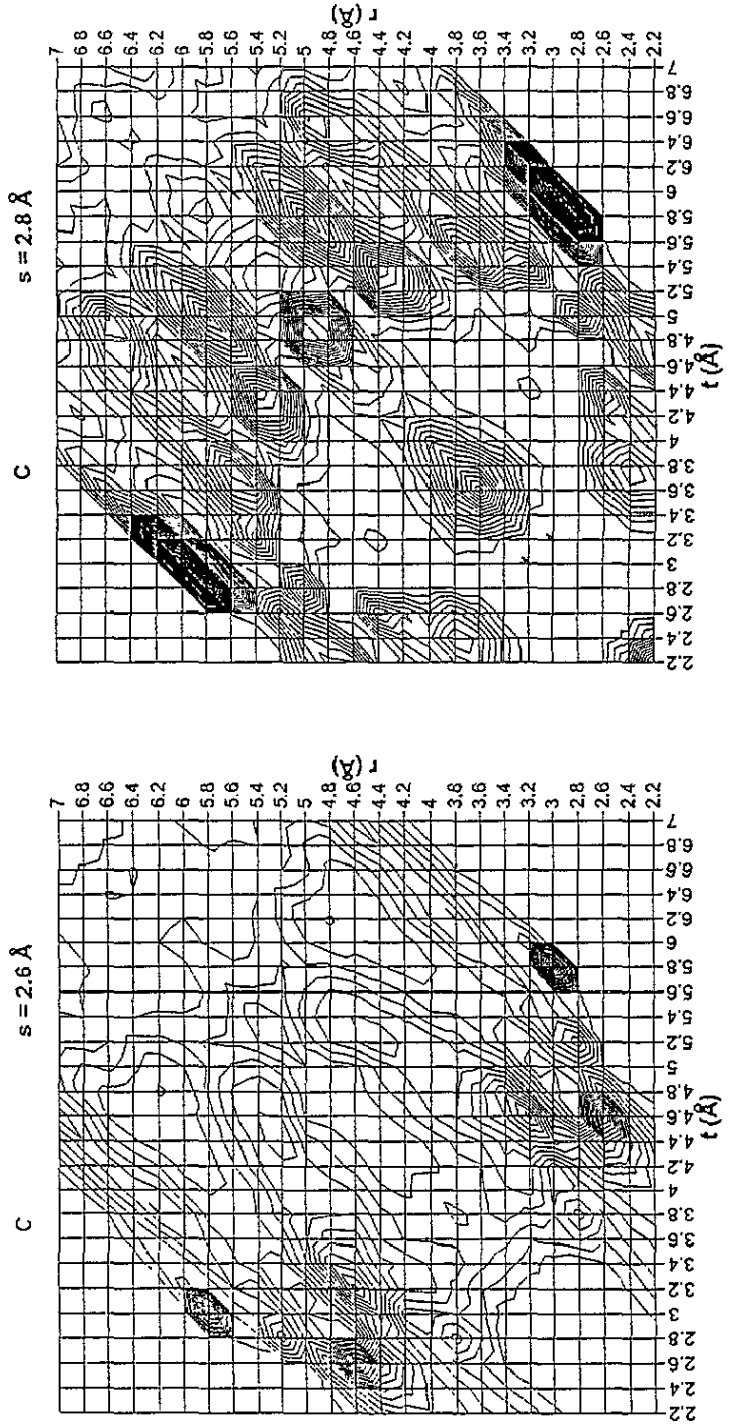


Figure 6. Continued.

On the other hand, concerning the reduced $g^{(3)}$ of model *C*, its resemblance to the corresponding full $g^{(3)}$ is striking: no additional feature can be seen on the reduced version. This is an extremely strong indication of the domination of higher-order (in this case three-body) correlations, which again connects model *C* with a crystalline-like structure.

Comparing the usefulness of the full and reduced $g^{(3)}$, no unambiguous assessment can be made about which one is the better. They can reveal different aspects of the atomic structure that can be equally important. As the main difficulty is the calculation of the full $g^{(3)}$, the normalization afterwards by the products of the appropriate $g^{(2)}$ being quick and easy, it is suggested that both should be applied for studying unknown structures.

As is evident from the above, all kinds of projections, apart from the isosceles (and equilateral) projections, of $g^{(3)}(r, s, t)$ give detailed and novel insights of the microscopic structure of disordered materials. They all are able to make the difference between structural models unambiguously, indicating also the extent of ordering that can be found in the models. Unfortunately, it is not possible to give a single number, or a few numbers, based somehow on $g^{(3)}$, as the measure of structural ordering. For this reason, two-dimensional projections of $g^{(3)}$ in themselves do not satisfy the final aim of the current study.

4.3. The three-body contribution to the configurational entropy, S_3

As was shown earlier [10, 11], S_3 can be derived from $g^{(3)}$ and $g^{(2)}$ quite readily. The comparison of S_3 for the three models can be seen in figure 1. As was discussed in [11], S_3 for model *U* behaves qualitatively differently from that of model *C*. As could be expected from the discussion in previous sections, S_3 of model *W* at short range (up to $r = 3.0 \text{ \AA}$, the boundary of the first coordination shell) goes with S_3 of model *C*. At higher distances the former does not follow with the dramatic fall of the latter, but behaves qualitatively similarly to S_3 of model *U*. These observations can fully be interpreted in terms of $g^{(3)}$. They are consistent with the crystalline-like peaks of $g^{(3)}$ of model *C* at higher distances, as well as with the presence (in model *U*) or the lack (in models *W* and *C*) of the 'hard-sphere'-like peak at $r = s = t = 2.2\text{--}2.4 \text{ \AA}$.

Note that the S_3 curves differ at around the first minimum of $g^{(2)}$, and later, from about the second peak of $g^{(2)}$, they are clearly separated. This makes S_3 a perfect and relatively simple tool for applying it as a quantitative measure of ordering. The lower (more negative) is S_3 , the higher is the degree of order in the given model. Comparing the values of S_3 at a specified r for different models can be simply that single number we have been looking for. The choice of the specified value is important but, since in this case the exact value of the configurational entropy is not looked for, it is important from a more technical point of view. According to this, it is advisable to choose an r value around which S_3 curves of the models studied are flat. In the present study, this r value can be about $r = 3.0 \text{ \AA}$.

4.4. The most probable structural model of amorphous silicon

While producing model *W* it was discovered that, of all the constrained RMC structural models we have produced so far [2, 3], the structure factor of model *W* best fitted the experimental $S(Q)$. (The difference from $S(Q)$ of model *C* is not clearly visible, but in terms of the sum of squared differences it is significant.) Furthermore, as seen from the study of $g^{(3)}$, model *W* does not possess the irrationally long-range structure, at least not at the level of three-body correlations, that so distinguished model *C*. Model *W*, as shown in figure 2, contains only tetrahedral angles, unlike model *U*. Considering these properties, it is suggested that model *W* could be the most appropriate structural model of amorphous silicon produced so far. The key to the model probably lies in the generation of the Wooten

model [13], where the initial bond switches prevent the structure from later going back to the diamond lattice.

It should be noted, however, that the above findings can only support what one would *expect* (in contrary to 'know' or 'measure') for amorphous silicon.

5. Conclusions

A number of tools applicable for distinguishing structures that are identical at the level of two-body correlations have been introduced and surveyed in detail. The most appropriate of them for measuring the degree of structural order/disorder seems to be the three-body contribution to the configurational entropy, S_3 . If simpler means are preferred, then the variance of the pair correlation function, $\Delta g^{(2)}$, is suggested for the same purpose, although it gives less resolved, and therefore more uncertain, information.

The three-particle correlation function, $g^{(3)}(r, s, t)$, proved to be an invaluable means of revealing details of the microscopic structure; $g^{(3)}$ was shown to easily separate models that looked identical at any level of geometrical analysis applied so far. Both the full and reduced $g^{(3)}$ could clearly resolve the difference between the models, but a short interpretation of them is lacking.

Model W, which is based on the Wooten model of amorphous silicon, is suggested to be the most appropriate structural model for a-Si.

Acknowledgments

This work has been supported by OTKA grants nos F4320 and F7218.

References

- [1] McGreevy R L and Pusztai L 1988 *Mol. Sim.* **1** 359
- [2] Kugler S, Pusztai L, Rosta L, Chieux P and Bellissent R 1993 *Phys. Rev. B* **48** 7685
- [3] Gereben O and Pusztai L 1994 *Phys. Rev. B* at press
- [4] McGreevy R L and Pusztai L 1990 *Proc. R. Soc. A* **430** 241
- [5] McGreevy R L, Howe M A, Keen D A and Clausen K 1990 *IOP Conf. Series* **107** 165
- [6] Baranyai A and Evans D J 1989 *Phys. Rev. A* **40** 3817
- [7] Green H S 1952 *The Molecular Theory of Fluids* (Amsterdam: North-Holland)
- [8] Nettleton R E and Green M S 1958 *J. Chem. Phys.* **29** 1365
- [9] Ravech  H J 1971 *J. Chem. Phys.* **55** 2242
- [10] Baranyai A and Evans D J 1990 *Phys. Rev. A* **42** 849
- [11] Gereben O, Pusztai L and Baranyai A 1994 *Phys. Rev. B* **49** 13251
- [12] Landau L D and Lifshitz E M 1981 *Theoretical Physics, vol. 5: Statistical Physics* (Budapest: Tankonyvkiad ) (in Hungarian)
- [13] Wooten F, Winer K and Weaire D 1985 *Phys. Rev. Lett.* **54** 1392
- [14] McNeil W J, Madden W G, Haymet A D J and Rice S A 1983 *J. Chem. Phys.* **78** 388
- [15] Pizio O and Pusztai L 1993 *Chem. Phys. Lett.* **214** 125